**PETROLEUM EXPLORATION AND DEVELOPMENT**
Volume 44, Issue 5, October 2017
Online English edition of the Chinese language journal

Available online at www.sciencedirect.com
ScienceDirect

**Cite this article as:** PETROL. EXPLOR. DEVELOP., 2017, 44(5): 720–730.

RESEARCH PAPER

# Characterization of micro-nano pore networks in shale oil reservoirs of Paleogene Shahejie Formation in Dongying Sag of Bohai Bay Basin, East China

HU Qinhong[1, 2,*], ZHANG Yuxiang[2], MENG Xianghao[3], LI Zheng[4], XIE Zhonghuai[4], LI Maowen[1]

1. State Key Laboratory of Shale Oil and Gas Enrichment Mechanisms and Effective Development, Research Institute of Petroleum Exploration and Production, Sinopec, Beijing 100083, China;
2. The University of Texas at Arlington, Arlington, Texas 76019, USA;
3. Chengdu University of Technology, Chengdu 610059, China;
4. Exploration and Production Research Institute of Shengli Oilfield Company, Sinopec, Dongying 257015, China

**Abstract:** For typical blocky, laminated and bedded mudrock samples from the Paleogene Shahejie Formation in the Dongying Sag of Bohai Bay Basin, this work systematically focuses on their structure characterization of multiple micro-nano pore networks. A use of mercury injection capillary pressure (MICP) documented the presence of multiple μm-nm pore networks, and obtained their respective porosity, permeability and tortuosity. Different sample sizes (500–841 μm GRI fractions, 1 cm-sized cubes, and 2.54 cm in diameter and 2–3 cm in height core plugs) and approaches (low-pressure $N_2$ gas physisorption, GRI matrix permeability, MICP, helium pycnometry, and pulse decay permeameter) were used to measure pore size distribution, porosity and permeability. The average porosity and matrix permeability determined from MICP are (6.31±1.64)% and $(27.4\pm31.1)\times10^{-9}$ μm$^2$, the pore throat diameter of pores is mainly around 5 nm, and the median pore throat diameter based on 50% of final cumulative volume is (8.20±3.01) nm in shale. The pore-throat ratios decrease with a decrease of pore size diameter. Moreover, the permeability of shale samples with lamination is nearly 20 times larger than matrix permeability. The geometrical tortuosity of the nano-scale 2.8–10.0 nm pore networks is 8.44 in these shales, which indicates a poor connectivity of matrix pore network and low flow capability. Overall, the variable and limited pore connectivity of shale samples will affect hydrocarbon preservation and recovery.

**Key words:** Bohai Bay Basin; Dongying Sag; Paleogene; shale oil; pore structure; porosity; permeability; connectivity; geometrical tortuosity

## Introduction

For the past decades shale formations have become major reservoirs, after sandstones and carbonates, for hydrocarbon (oil and gas) exploration and development. Since 2005 when China initiated shale gas development, rapid advances in the theories and technologies have been achieved for a successful commercial development in 2014. At present, shale gas development has been systematically progressing towards large-scale production in marine shales, and industrialization in lacustrine and transitional shales[1]. However, progresses in shale (tight) oil development have been very slow. Focusing on core samples of Shahejie Formation (the exploration target for shale oil) of Dongying Sag in Jiyang Depression of Bohai Bay Basin in East China, this study employs high-pressure mercury injection capillary pressure (MICP) to characterize multiple connected pore networks at μm-nm scales, and analyze the proportion, as well as porosity and permeability, of each connected pore network. The MICP results are compared with pore-size distribution from low-pressure $N_2$ physisorption and matrix permeability from GRI (Gas Research Institute) method, in terms of measurement principles and sample sizes. The overall results implicate a low pore connectivity of shales in influencing oil recovery.

## 1. Regional geology and sample collection

The Jiyang Depression is located in the southeastern part of the Bohai Bay Basin. It is bounded by the Tanlu Fault to the east, Luxi Uplift to the south, and Chengning Uplift to the north and west[2–3]. Covering approximately $2.65\times10^4$ km$^2$, the Jiyang Depression is comprised of four sub-depressions from

**Received date:** 13 Feb. 2017; **Revised date:** 15 Jul. 2017.
*** Corresponding author.** E-mail: water19049@gmail.com
**Foundation item:** Supported by the National Key Basic Research and Development Program (973 Program) in China (2014CB239100) and the Foundation of State Key Laboratory of Shale Oil and Gas Enrichment Mechanisms and Effective Development (No. G5800-15-ZS-WX051) at Petroleum Exploration and Production Research Institute of Sinopec, China.

south to north (named Dongying, Huimin, Chezhen and Zhuanhua sags), as well as several bulges separating these sags. The Dongying Sag, located to the south of the Jiyang Depression, is one of the 3rd-order negative tectonic units of Cenozoic rift basins in the Bohai Bay Basin. With a length of 90 km in EW direction and 65 km in SN for an exploration area of about 5 760 $km^2$[4], the Dongying Sag consists of four sub-sags with hydrocarbon soruce rocks: Lijin, Boxing, Niuzhuang, and Minfeng, as well as several 2nd-order tectonic units, including the northern steep slope zone, central anticlinal zone, and southern gentle slope zone (Fig. 1).

The Neogene is the most important filling period for the Dongying Sag, with a sedimentary layer up to 7 km. With a wide distribution, the Paleogene is composed of, from bottom to top, Kongdian, Shahejie, and Dongying Formations. Among these formations, the Shahejie Formation has the widest distribution, and is made of $Es^1$, $Es^2$, $Es^3$ and $Es^4$ members from top to bottom. Vertically, the main oil-producing zones are lower $Es^3$ and upper $Es^4$ sub-members[2]. The upper $Es^4$ sub-member is comprised of gray conglomerate with interbedded mudrock at multiple depositional stages, while lower $Es^3$ sub-member is well developed with widely- distributed lacustrine dark-colored (brown and gray) mudrocks, oil shales, marls, and other lithologies at a thickness of 100–300 m[3].

A systematic shale coring well by Shengli Oil Field, Liye #1 well is situated in about 200 m northwest of Shangjia Village, Longju Sub-district, Niuzhuang District in Kenli County of Sangdong Province. Completed in October of 2012, the total depth is 3 924.00 m in lower $Es^4$ sub-member. It is targeted for lower $Es^3$ and upper $Es^4$ sub-members, with some coverage for middle $Es^3$ sub-member, the coring depths are located at 3 580.00–3 695.48 m (lower $Es^3$—upper $Es^4$) and 3 735.00–3 835.08 m (upper $Es^4$) below the ground surface, with a total coring length of 215.58 m[5]. Table 1 presents three core samples, used in this work, with different litho-facies from lower $Es^3$ and upper $Es^4$ sub-members. Various sub-samples are processed from the core samples for the following different and complementary tests: 2.54 cm in diameter by 2.0–3.3 cm high core plugs cored at both parallel and transverse to the bedding plane (for helium porosity-permeability analyses), 1-cm-sided cubes (for MICP), GRI size fractions of 500–841 μm (for matrix permeability), and powder size fractions of < 75 μm (for XRD mineralogy, total organic carbon TOC, and vitrinite reflectance $R_o$).

## 2. MICP analyses

For a cubic shale sample with 1 cm on each side, the MICP technique is used to characterize pore structure, including the skeletal and bulk densities, porosity, pore-throat size distribution, pore surface area, permeability, and tortuosity, using a mercury intrusion porosimeter (AutoPore IV 9510, Micromeritics Instrument Corporation, Norcross, GA, USA). The MICP method is applicable to the analysis of connected pore spaces with a range of 2.8 nm–50 μm in pore-throat diameters, based on a penetrometer[6] suitable for shale samples with a porosity of about 0.1%–5.0%. This pore-size measurement range is wider than that of low-pressure $N_2$ physisorption, and in addition, MICP analysis can yield other pore structure parameters such as specific surface area, permeability and tortuosity[7].

As a non-wetting fluid with respect to most porous materials, mercury (with a molecular size of 0.31 nm) does not spontaneously enter the pore space of shale. Pressurizing the mercury forces it to enter the pores and higher pressure is required to invade smaller pore-throats; hence, MICP approach can produce mercury intrusion curves by accurately detecting the volume change of mercury under each pressure. Wang et al. (2016)[8] reported that, pore-sizes calculated with

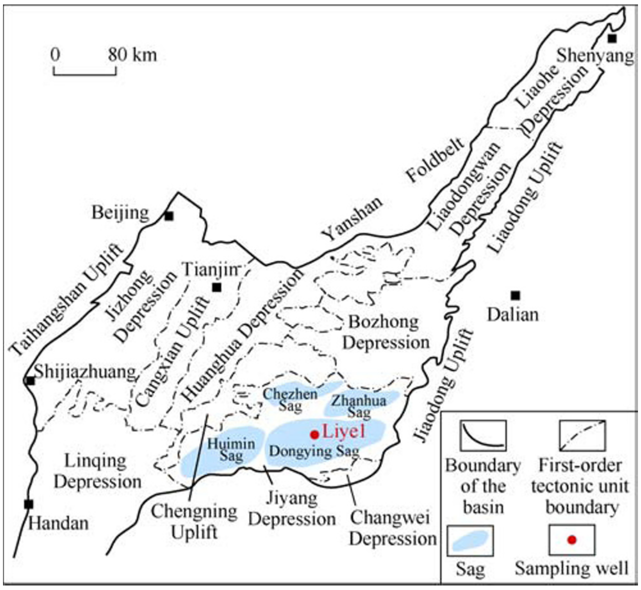


**Fig. 1. Location of the study area.**

**Table 1. Basic properties and mineral composition of shale samples from the Paleogene Shahejie Formation in Liye #1 well**

| Sample | Depth / m | Sub-member | Lithology | $R_o$/ % | TOC/ % | Quartz/ % | Plagioclase/% | Albite/% | Calcite / % | Dolomite/% | Pyrite/ % | Siderite/ % | Illite/ % | Illite-smectite mixed layer/% | Kaolinite/% |
|---|---|---|---|---|---|---|---|---|---|---|---|---|---|---|---|
| Liye-61 | 3 595.11 | Lower $Es^3$ | Bedded calcareous shale | 0.52 | 2.11 | 22.0±0.6 | 6.3±0.7 | 15.2±2.0 | 13.4±0.5 | 10.9±0.6 | 2.3±0.1 | 2.7±0.3 | 6.8±1.0 | 16.8±1.2 | 3.6±0.7 |
| Liye-481 | 3 752.56 | Upper $Es^4$ | Blocky calcareous shale | 0.64 | 1.42 | 22.1±0.7 | 0.5±0.4 | 9.2±1.9 | 21.1±0.7 | 6.3±0.5 | 1.5±0.4 | 1.2±0.7 | 11.4±0.9 | 26.6±2.8 | |
| Liye-603 | 3 782.63 | Upper $Es^4$ | Laminated calcareous shale | 0.74 | 2.83 | 35.6±0.9 | 2.5±0.6 | 5.6±1.6 | 26.5±0.7 | 5.7±0.5 | 2.0±0.5 | 0.5±0.5 | 7.5±0.7 | 13.1±1.5 | |